Published in final edited form as:
J Am Chem Soc. 2013 March 6; 135(9): 3339–3342. doi:10.1021/ja311588c.

Synthesis of Nanostructured and Biofunctionalized Water-in-Oil Droplets as Tools for Homing T Cells

Ilia Platzman[‡], **Jan-Willi Janiesch**[‡], and **Joachim Pius Spatz**[*]
Department of New Materials and Biosystems, Max Planck Institute for Intelligent Systems, Heisenbergstr. 3, 70569 Stuttgart, Germany & Department of Biophysical Chemistry, University of Heidelberg, 69120 Heidelberg, Germany

Abstract

Activation, *ex-vivo* expansion of T cells, differentiation into a regulatory subset and its phenotype specific high-throughput selection represent major challenges in immunobiology. In part, this is due to the lack of technical means to synthesize suitable 3-D extracellular systems to imitate *ex-vivo* the cellular interactions between T cells and antigen presenting cells (APC). In this study, we synthesized a new type of gold-linked surfactants and used a drop-based microfluidic device to develop and characterize novel nano-structured and specifically biofunctionalized droplets of water in oil emulsions as 3-D APC analogues. Combining flexible biofunctionalization with the pliable physical properties of the nanostructured droplets provides this system with superior properties in comparison to previously reported synthetic APC analogs.

Interactions of T cells and antigen-presenting cells (APC) play a crucial role in orchestrating the body's adaptive immune and inflammatory responses to pathogens and mutations. The fate of T cells is exquisitely regulated not only by the presence of certain molecules on the surface of APC, but also by their density and spatial distribution on the nanometric scale.[1–6] Moreover, properties such as the elasticity and curvature of both T cells and APC, in addition to the force-dependent conformational changes during the formation of the immunological synapse (IS) (i.e. the T cell-APC interface), may play a crucial role in the regulation of T cells' fate.[7–12] Recent preclinical studies indicate that adoptive transfer of regulatory T cells (Treg) can exhibit marked beneficial impact on different autoimmune diseases.[13–15] Therefore, the induction and *ex vivo* expansion of T cells in general represents a major challenge due to the difficulty of simulating *in vitro* the intimate cellular interaction between the T cell receptors (TCR) and the target APC as it occurs in peripheral lymphoid organs.[5] In part, this difficulty is associated with the lack of technical means to develop suitable 2-D and especially 3-D artificial APC analogues.

During the last decade much effort has been concentrated on the development of 2-D APC analogues. The most common technology was based on supported lipid bilayers, which can provide a model system for mimicking the cell membrane as the lateral mobility of lipids and proteins resembles qualitatively the *in vivo* situation. Moreover, many surface

Corresponding Author: spatz@is.mpg.de.
‡**Author Contributions**
These authors contributed equally.

The authors declare no competing financial interests.

Supporting Information
Experimental details for the synthesis of the surfactants, descriptions of the microfluidic device, droplet creation, collection and storage, experimental details for cell adhesion experiments, FTIR spectra and their characterization, cryo-SEM micrographs of droplets, and fluorescence microscopy images. This material is available free of charge via the Internet at http://pubs.acs.org."

patterning techniques have been used to define certain spatial constraints within a lipid bi-layer to alter the mobile fraction of functionalized proteins.[16–18] However, only a few techniques such as dip-pen,[19] e-beam lithography[20] and block copolymer micelle nanolithography (BCML)[21] were able to achieve patterns with sub-100 nm spatial resolution, a length scale which plays a significant role in T cell activation.[4] Despite the versatility of these systems, only partial success was achieved in mimicking the T cell – APC interaction as it occurs *in vivo*.[7,22] The ability of these systems to serve as an optimal APC analog is mainly hindered by the lack of mechanosensing capabilities during the IS formation due to the rigid materials and planar system structure.[7,23,24]

Mono-disperse polystyrene beads of 5–6 μm in diameter endowed with antibodies or other proteins heralded another area of synthetic APC which considered to more closely imitating the cellular interactions between T cells and APC than planar systems.[25] However, the limitation of bead-based artificial APC is in incompatibility of the system towards dynamic remodeling of the proteins that is established at the IS between the professional APC and T cells.

Drops of water-in-fluorocarbon emulsions created in a drop-based microfluidic device have been tested and used recently as 3-D scaffolds for *in vitro* translation, encapsulation and incubation of cells.[26–30] Non-ionic fluorosurfactants made of perfluorinated polyethers (PFPE) (hydrophobic tails) provide long term stability to the drops by preventing coalescence, while polyethylene glycol (PEG) moieties (hydrophilic headgroups) serve as a biocompatible, inert interior surface of the water drops.[26] The flexible design of the microfluidic device allows for the creation of drops with different diameters, easily varied from 10 μm, the required minimum for single cell encapsulation, upward.[31] The softness of the droplet walls can be efficiently controlled by varying the surfactant concentration prior to droplet formation. Therefore, the change in droplet diameter and consequent change in the curvature, together with the soft nature of this system, increase the potential of this system to confer the key physical functions of native APC. However, the current state of the art emulsion systems fail to provide the required chemical and biological functions of the APC.

In the present study, we provide a novel approach that merges nano-patterning and droplet microfluidics to develop an APC 3-D analog with a well-defined chemical and physical microenvironment. This important challenge is addressed in this study by developing and characterizing novel gold nanostructured and specifically biofunctionalized drops of water in oil emulsion, as schematically illustrated in Figure 1. The gold nanoparticles were used in this study as anchoring points for bio-active molecules, which are required for cell interactions. Additionally, these nanoparticles allowed for qualitative and quantitative characterization of the droplets with high resolution cryo scanning electron microscopy (cryo-SEM).

Synthesis of the PFPE-PEG-PFPE triblock-copolymer surfactants (Figure 1B) followed the procedure reported earlier[26] but with several modifications such as using a one-step condensation reaction between PEG600-diol and PFPE2500-carboxylic acid (see Supporting Information (SI), Section 1.1). Gold-linked surfactants (30 μM) (Figure 1 C) were synthesized using one-step condensation reaction between PFPE7000-carboxylic acid and (11-Mercaptoundecyl)tetra(ethyleneglycol) functionalized gold nanoparticle solution (see SI, Section 1.2). Nuclear magnetic resonance (NMR) and Fourier transform infrared (FTIR) spectroscopies were used to confirm the success of the surfactants' syntheses and their purities (see SI, Sections 1.1 and 4.1, respectively).

A droplet-based microfluidic device made of PDMS was used to create the water in oil emulsion droplets (see SI, Section 2). Triblock PFPE-PEG-PFPE and diblock PFPE-PEG-

Gold surfactants were mixed with different concentration ratios in order to get stable emulsion droplets with varied gold nanoparticles densities. To verify the successful creation of the nanostructured droplets, the droplets were freeze fractured and investigated by cryo-SEM (see SI, Section 4.2). Figure 2 shows representative cryo-SEM (top view) micrographs of the freeze fractured nanostructured droplets which were created using different concentrations of the gold-linked surfactants (30 μM A and B, 3 μM C and D). The gold nanoparticles of ~5 nm in diameter are presented on the inner periphery of the droplet. A higher density of the gold nano-particles and their more homogeneous distribution can be observed on the droplets obtained with a higher concentration (30 μM) of the gold-linked surfactants (Figure 2B). To prove that the bright dots are gold nanoparticles and not artifacts due to the cryo-SEM measurements or freeze fracture preparation, droplets without gold-linked surfactants were created, freeze fractured and observed by cryo-SEM (see SI, Section 4.2, Figures 10S A and B).

The ability of the gold nanoparticles in the nanostructured droplets to serve as anchoring points towards future biofunctionalization was tested with two different approaches: The first approach was based on functionalization of the created nanostructured droplets with His6-GFP via a NTA-Thiol linker (see SI, Sections 1.4 and 4.3.1). Successful functionalization of the nanostructured droplets with His6-GFP is particularly important, since the chemistry behind the immobilization of these proteins is the same as is required for immobilization of the peptide-loaded major histo-compatibility complexes (pMHC) or proteins such as aCD3 or aCD28, which are important in T cell activation.[32] The second, two-step approach contained as a first step synthesis of PFPE-PEG-Gold surfactants linked to Rhodamine B (RhB) (see SI, Section 1.3), and as a second step creation of RhB-linked nanostructured droplets (see SI, Section 4.3.2).

For the first approach, the freshly prepared phosphate buffered saline (PBS) solution of His6GFP-Ni-NTA-Thiol (8 μM) was used as aqueous phase to create droplets in a microfluidic device. Two types of droplets were investigated; those containing only PFPE-PEG-PFPE (20 mM) surfactants and another containing a mixture of PFPE-PEG-PFPE (20 mM) and Gold-PEG-PFPE (30 μM) surfactants in the oil phase. Figure 3 (A, B and C) shows fluorescence images of the His6GFP-Ni-NTA-linked nanostructured droplets, taken one day, four days and ten days after creation, respectively. It can be seen that the fluorescence is concentrated on the periphery of the droplets. The decrease in the fluorescence intensity after four days can be explained by the dilution of the GFP in the droplets periphery due to the oxidation of the gold-sulphur bond in the aqueous phase[33] and following diffusion to the oil phase. In the oil phase, the GFP lose their fluorescent properties due to the solvent-induced denaturation.[34] In comparison to nanostructured droplets, the fluorescence intensity in the droplets without gold nanoparticles was distributed equally inside the droplets (see SI, Figure 11S A). The same, equal distribution was observed in the nanostructured droplets where the His6GFP (8 μM) was used without the NTA-thiol linker (see SI, Figure 11S B).

To create RhB-linked nanostructured droplets, the mixture of PFPE-PEG-PFPE (20mM) and RhB-PEG-Gold-PEG-PFPE (30 μM) surfactants was used as an oil phase and PBS was used as an aqueous phase. Figure 4 (A, B and C) shows representative fluorescence images of the RhB-linked nanostructured droplets taken after one, seven and sixteen days, respectively. Due to the chemical bonding of the RhB to the Gold-PEG-PFPE-surfactants, the fluorescence signal is observed on the droplet's periphery and it is stable over two weeks. Better stability in comparison to GFP-linked droplets can be attributed to the larger number of RhB molecules per gold nanoparticle due to the lower steric hindrance, and the generally higher fluorescence stability of RhB in comparison to GFP. Additionally, a homogeneous distribution of the fluorescence signal on the droplet periphery along the RhB-linked

nanostructured droplet height was observed by z-stack confocal microscopy (see SI, Section 4.3.2).

The successful creation of functionalized droplets using a two-step approach widens the possibilities of the nanostructured droplets system towards biofunctionalization. Moreover, it allows for the creation of biofunctionalized droplets with no soluble bio-active molecules in an aqueous phase, which could potentially block active sites on the cell surface, and consequently prevent cell-droplets interactions. Inspired by this achievement, we used the human acute T cell leukemia cell line (Jurkat E6.1) to assess the ability of the nanostructured and biofunctionalized droplets to serve as potential 3-D APC analog system. Jurkat T cells express the $\alpha_4\beta_1$ and $\alpha_5\beta_1$ integrins and exhibit activation-dependent regulation of integrin-mediated adhesion.[35] Therefore, to provide cell interactions with nanostructured droplets, cyclic arginine-glycine-aspartic acid peptide c(RGDfK)-PEG6-cysteine was immobilized on gold-PEG-PFPE surfactants via the thiol residue of the cysteine (see SI, Section 1.5).[36] The peptide is specific against $\alpha_5\beta_1$.

For cell adhesion experiments, a mixture of PFPE-PEG-PFPE (20 mM) and RGD-gold-PEG-PFPE (25 μM) surfactants was used to create biofunctionalized droplets. Jurkat E6.1 cells (6×10^6 cells) were suspended in adhesion medium which was used as an aqueous phase (see SI, Sections 2 and 3). Figure 5 shows a representative droplets ensemble with the encapsulated Jurkat T cells (indicated by arrows). Strikingly, after one hour of incubation ~90 % of cells were observed to be in contact with the droplet's periphery (Figure 5 B). However, the cells encapsulated inside droplets without RGD-linked surfactants remained randomly distributed along the droplets, similar to our previous observations.[29] The number of cells per droplet could be controlled by varying the initial number of cells added to the microfluidic channel. The cells demonstrated viability up to 5 days incubation (see SI, Section 3.2). This observation aligns well with the previously reported results which showed Jurkat cells viability up to 9 days encapsulation in the 100 μm droplets made of triblock surfactants.[30] Shorter viability period as observed in this study is most likely due to the 20-fold smaller droplets volume, consequently lack of nutrition.

To further investigate the cell-droplet interaction with high resolution, the cells containing droplets were freeze-fractured and investigated by cryo-SEM (see SI, Section 4.2). Viewed by cryo-SEM at different magnifications (Figure 6 A–D), all cells are spherical having diameters ranging from 3 to 5 μm, similar to previous observations.[37,38] Confirming the brightfield microscopy observations, cell-droplet periphery interactions can be easily observed.

In conclusion, we have synthesised and developed gold-nanostructured and specifically biofunctionalized drops of water in oil emulsion which has a potential to serve as 3-D APC analogues. The efficiency of the gold nanoparticles in the nanostructured droplets to provide the required chemical and biological key functions of the APC was presented and tested. Combining flexible biofunctionalization with the pliable physical properties of the nanostructured droplets can play a crucial role as it results in a flexible and modular system that closely models *in situ* APC-T cell interactions. Consequently, these systems will contribute to the understating if the force-dependent conformational changes during IS formation playing a role in the transduction of co-stimulatory signals in T cells during the process of T cell activation. The ability of T cells to exert forces in all 3 dimensions on the bio-molecules held by the drop may also be important in evaluating the affinity and function of antigen receptors which is not the case with T cells studies on supported surfaces or bead-based APC.[7,12,25,39]

Supplementary Material

Refer to Web version on PubMed Central for supplementary material.

Acknowledgments

I.P. gratefully acknowledges the support of the Alexander von Humboldt Foundation. Part of the research leading to these results has received funding from the European Union Seventh Framework Programme (FP7/2007-2013) under grant agreement n° NMP4-LA-2009-229289 NanoII and n° NMP3-SL-2009-229294 NanoCARD. This work is also part of the excellence cluster CellNetwork at the University of Heidelberg and the National Institutes of Health (NIH) Common Fund Nanomedicine program (PN2 EY016586). J.P.S. is the Weston Visiting Professor at the Weizmann Institute of Science. The authors are indebted to Dr. Claire Cobley and Dr. Markus Axmann for detailed revision of the manuscript and to Dr. Christian Boehm for fruitful discussions. We are also indebted to Professor Yeshayahu Talmon (Technion, Israel) for sharing with us his experience of conducting the cryo-SEM measurements.

References

1. Alberts, B.; Johnson, A.; Lewis, J.; Ralf, M.; Roberts, K.; Walter, P. Molecular biology of the cell. 4. Garland Science, a member of the Taylor & Francis Group; New York: 2002.
2. Geiger B, Spatz JP, Bershadsky AD. Nature Rev Mol Cell Biol. 2009; 10:21.
3. Giannoni F, Barnett J, Bi K, Samodal R, Lanza P, Marchese P, Billetta R, Vita R, Klein MR, Prakken B, Kwok WW, Sercarz E, Altman A, Albani S. J Immunol. 2005; 174:3204. [PubMed: 15749850]
4. Lillemeier BF, Mortelmaier MA, Forstner MB, Huppa JB, Groves JT, Davis MM. Nature Immunol. 2010; 11:90.
5. Manz BN, Groves JT. Nature Reviews Molecular Cell Biology. 2010; 11:342.
6. Vrljic M, Nishimura SY, Brasselet S, Moerner WE, McConnell HM. Biophys J. 2002; 83:2681.
7. Alon R, Dustin ML. Cell Press. 2007; 26:17.
8. Huppa JB, Davis MM. Nature Immunol. 2003; 3:973.
9. Lee K, Holdorf AD, Dustin ML, Chan AC, Allen PM, Shaw AS. Science. 2002; 295:1539.
10. Moss WC, Irvine DJ, Davis MM, Krummel MF. PNAS. 2002; 99:15024.
11. Sakaguchi S, Sakaguchi N. Int Rev Immunol. 2005; 24:211.
12. Varma R, Campi G, Yokosuka T, Saito T, Dustin ML. Immunity. 2006; 25:117.
13. Tang Q, Henriksen KJ, Bi M, Finger EB, Szot G, Ye J, Masteller EL, McDevitt H, Bonyhadi M, Bluestone JA. J Exp Med. 2004; 199:1455.
14. Tarbell KV, Petit L, Zuo X, Toy P, Luo X, Mqadmi A, Yang H, Suthanthiran M, Mojsov S, Steinman RM. J Exp Med. 2007; 204:191. [PubMed: 17210729]
15. Haile LA, Von WR, Gamrekelashvili J, Kruger C, Bachmann O, Westendorf AM, Buer J, Liblau R, Manns MP, Korangy FFGT. Gastroenterology. 2008; 135:871. [PubMed: 18674538]
16. Jackson BL, Groves JTJ. Am Chem Soc. 2004; 126:13878.
17. Mossman KD, Campi G, Groves JT, Dustin ML. Science. 2005; 310:1191. [PubMed: 16293763]
18. Groves JT, Ulman N, Boxer SG. Science. 1997; 275:651. [PubMed: 9005848]
19. Lenhert S, Sun P, Wang YH, Fuchs H, Mirkin CA. Small. 2007; 3:71. [PubMed: 17294472]
20. Shen KY, Tsai J, Shi P, Kam LCJ. Am Chem Soc. 2009; 131:13204.
21. Spatz, JP.; Geiger, B. In Methods in Cell Biology. YuLi, W.; Dennis, ED., editors. Vol. 83. Academic Press; 2007. p. 89
22. Hosseini BH, Louban I, Djandji D, Wabnitz GH, Deeg J, Bulbuc N, Samstag Y, Gunzer M, Spatz JP, Hammerling GJ. PNAS. 2009; 106:17852. [PubMed: 19822763]
23. Judokusumo E, Tabdanov E, Kumari S, Dustin ML, Kam LC. Biophysical Journal. 2012; 102:L5. [PubMed: 22339876]
24. O'Connor RS, Hao XL, Shen KY, Bashour K, Akimova T, Hancock WW, Kam LC, Milone MC. Journal of Immunology. 2012; 189:1330.
25. Turtle CJ, Riddell SR. Cancer J. 2010; 16:374.

26. Holtze C, Rowat AC, Agresti JJ, Hutchison JB, Angile FE, Schmitz CHJ, Köster S, Duan H, Humphry KJ, Scanga RA, Johnson JS, Pisignano D, Weitz DA. Lab Chip. 2008; 8:1632. [PubMed: 18813384]
27. Rowat AC, Bird JC, Agresti JJ, Rando OJ, Weitz DA. PNAS. 2009; 106:18149. [PubMed: 19826080]
28. Schmitz CHJ, Rowat AC, Köster S, Weitz DA. Lab Chip. 2009; 9:44. [PubMed: 19209334]
29. Hofmann TW, Anselmann SH, Janiesch JW, Rademacher A, Bohm CHJ. Lab on a Chip. 2012; 12:916.
30. Clausell-Tormos J, Lieber D, Baret JC, El-Harrak A, Miller OJ, Frenz L, Blouwolff J, Humphry KJ, Koster S, Duan H, Holtze C, Weitz DA, Griffiths AD, Merten CA. Chem Biol. 2008; 15:427.
31. Shah RK, Shum HC, Rowat AC, Lee D, Agresti JJ, Utada AS, Chu LY, Kim JW, Nieves A, Martinez CJ, Weitz DA. Materialstoday. 2008; 11:18.
32. Dustin ML. Immunol Rev. 2008; 221:77. [PubMed: 18275476]
33. Vericat C, Vela ME, Benitez G, Carro P, Salvarezza RC. Chem Soc Rev. 2010; 39:1805. [PubMed: 20419220]
34. Ward, WW.; Chalfie, M.; Kain, SR., editors. John Wiley & Sons, Inc; New Jersey: 2006.
35. Romzek NC, Harris ES, Dell CL, Skronek J, Hasse E, Reynolds PJ, Hunt SW, Shimizu Y. Mol Biol Cell. 1998; 9:2715. [PubMed: 9763439]
36. Barczyk M, Carracedo S, Gullberg D. Cell and tissue research. 2010; 339:269.
37. Zhang CG, Xu YH, Gu JJ, Schlossman SF. PNAS. 1998; 95:6290. [PubMed: 9600958]
38. Majstoravich S, Zhang JY, Nicholson-Dykstra S, Linder S, Friedrich W, Siminovitch KA, Higgs HN. Blood. 2004; 104:1396. [PubMed: 15130947]
39. Grakoui A, Bromley SK, Sumen C, Davis MM, Shaw AS, Allen PM, Dustin ML. Science. 1999; 285:221.

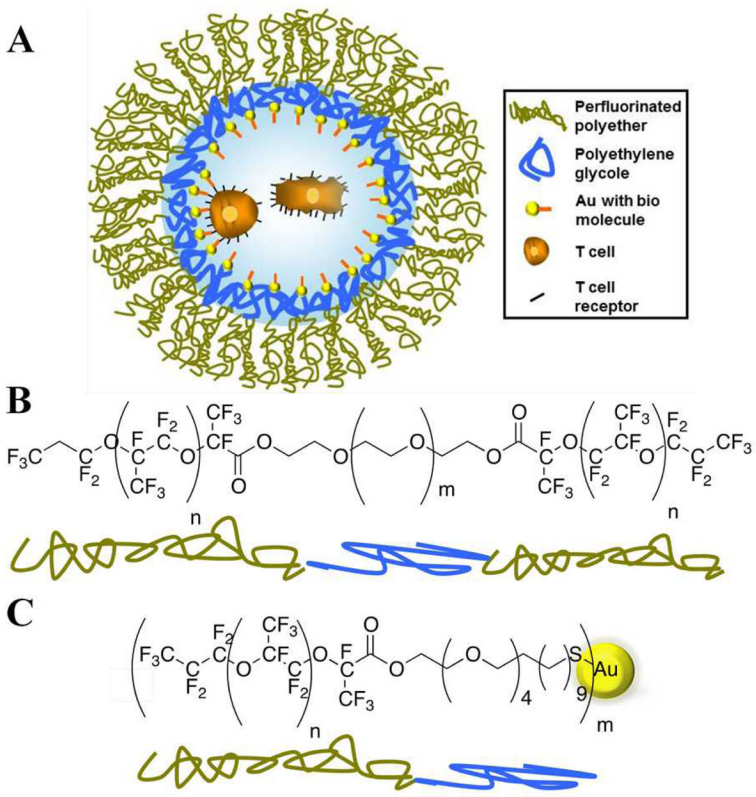

Figure 1.

A) Schematic representation of the nanostructured and specifically biofunctionalized drop of water-in-oil emulsion as a 3-D APC analog. Two encapsulated T cells are schematically shown inside the drop. This schematic representation is not to scale. B) and C) present the synthesized PFPE-PEG triblock copolymers and PFPE-PEG-Gold diblock surfactants, respectively.

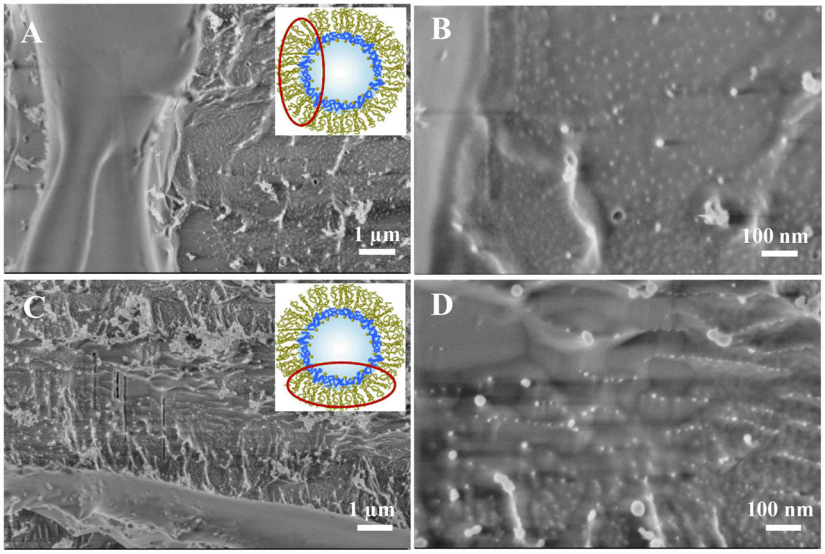

Figure 2.

Cryo-SEM, representative micrographs of the freeze fractured nanostructured droplets, obtained with different magnifications. In A) and B) the droplets were created using a Gold-PEG-PFPE concentration of 30 μM, in C) and D) the concentration was 3 μM. All droplets were created using 20 mM PFPE-PEG-PFPE triblock copolymer surfactants. For clarity, the insets show the schematic representation of the droplet and the area of observation (not to scale).

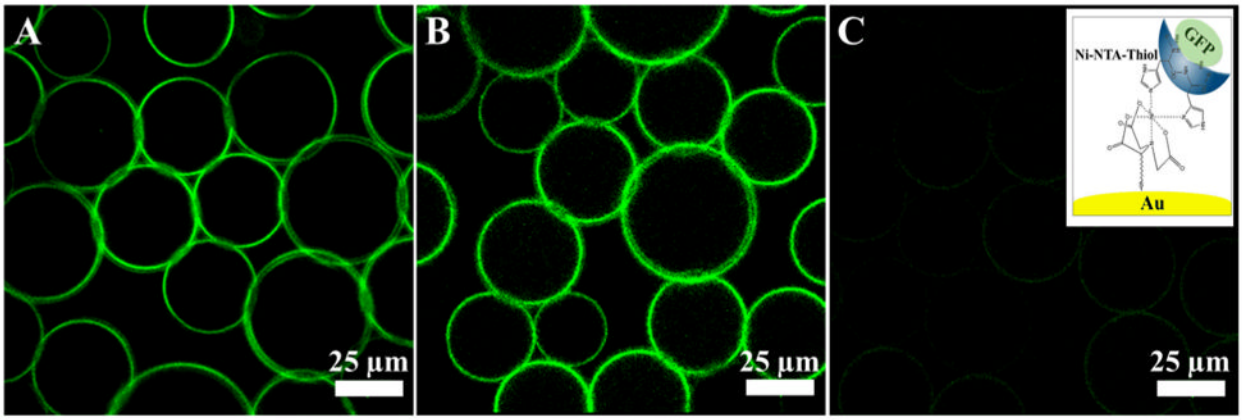

Figure 3.

Representative, fluorescent images of the GFP-linked gold-nanostructured droplets, measured (A) 1 day, (B) 4 days and (C) 10 days after creation, respectively. All images have the same intensity scale. The right inset shows the chemical immobilization of the His6-GFP on top of the gold nanoparticle by means of Ni-NTA-thiol linker (not to scale).

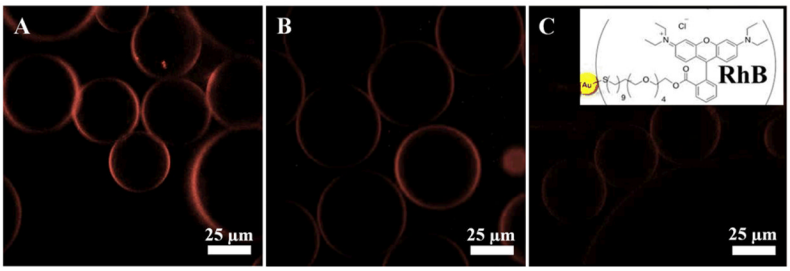

Figure 4.
Representative fluorescent images of the RhB-linked gold-nanostructured droplets, measured (A) one day, (B) seven days and (C) sixteen days after creation, respectively. All images have the same intensity scale. The right inset shows the chemical immobilization of the RhB on top of the gold nanoparticle (not to scale).

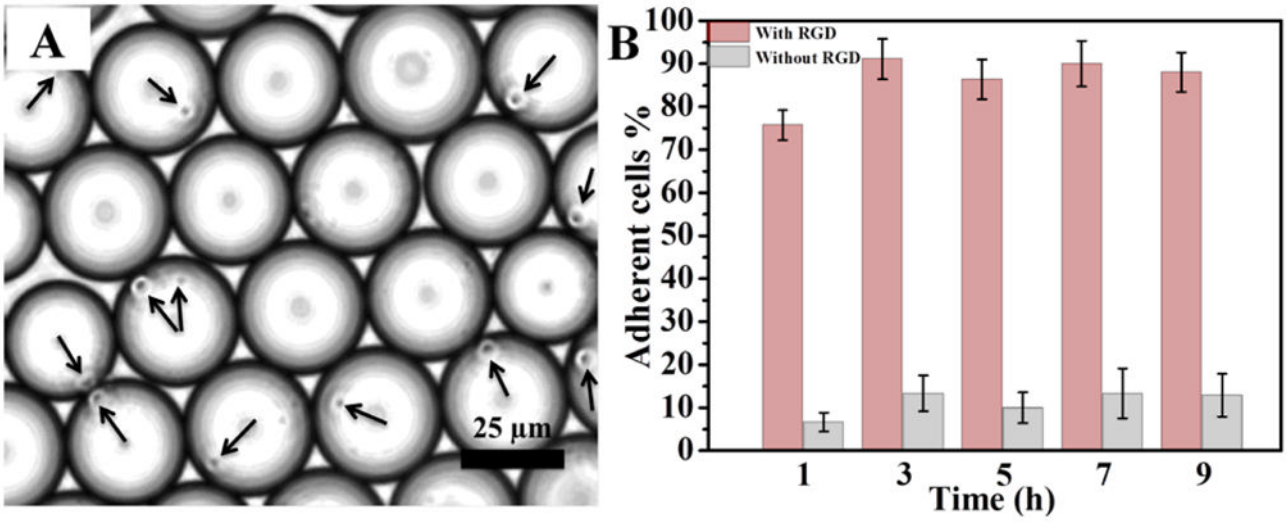

Figure 5.

A) Brightfield, representative image of Jurkat E6.1 cells (indicated by arrows) in the cRGD-functionalized nanostructured droplets 6 h after creation. B) Quantification (adherent cells %) of Jurkat E6.1 cell adhesion on nanostructured and cRGD functionalized (pink, left bars) and non-functionalized (grey, right bars) droplets. Data is presented as mean ± s.e.m., n=5.

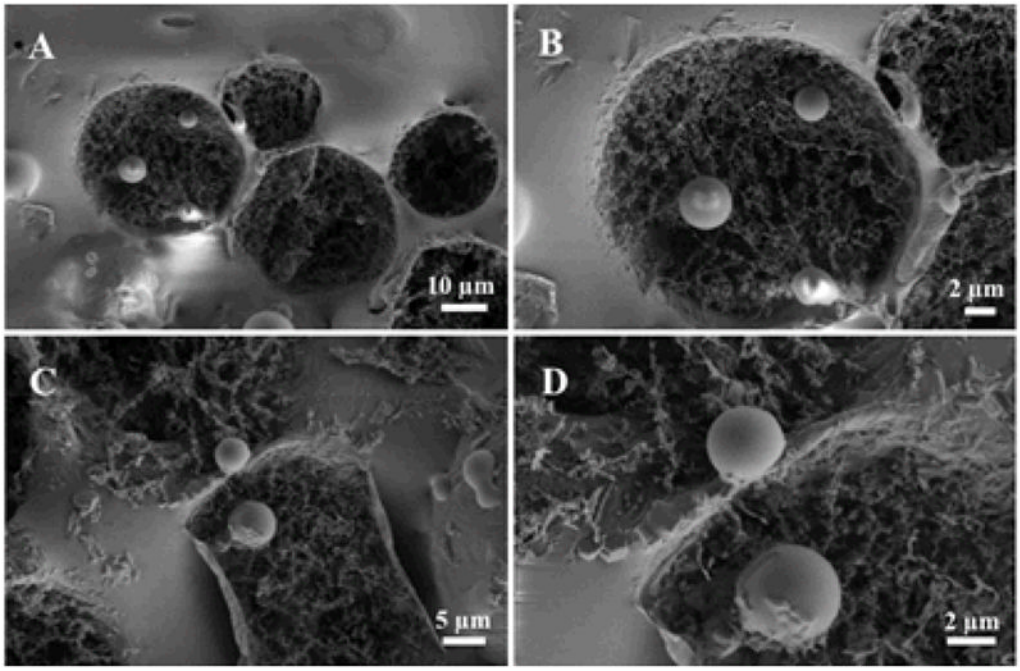

Figure 6.
Cryo-SEM, representative micrographs of the freeze-fractured, biofunctionalized droplets after the Jurkat E6.1 cell adhesion experiment.